Electronic Supplementary Material (ESI) for Inorganic Chemistry Frontiers.


**Supporting information**

# Low-content Ru-Pt Supported On Oxygen Vacancy Enriched Black $TiO_2$ with Strong Electronic Interactions as Efficient Hydrogen Generation Electrocatalysts

*Yuanzong Shen [c], Weichen Li [a], Wenna Wang [a] Liantao Xin [a], Weiping Xiao [b], Guangrui Xu [d], Dehong Chen [d], Lei Wang [a], Fusheng Liu [*c], Zexing Wu [*a]*

a. Key Laboratory of Eco-chemical Engineering, Ministry of Education, International Science and Technology Cooperation Base of Eco-chemical Engineering and Green Manufacturing, College of Chemistry and Molecular Engineering, Qingdao University of Science and Technology, Qingdao 266042, Shandong, China E-mail: splswzx@qust.edu.cn; inorchemwl@126.com.

b. College of Science, Nanjing Forestry University, Nanjing 210037, Jiangsu, China.

c. College of Chemical Engineering, Qingdao University of Science and Technology, Qingdao 266042, China.

d. School of Materials Science and Engineering, Qingdao University of Science and Technology, Qingdao 266042, Shandong, China.

## Experimental Section

**Preparation of Ru-Pt/P-$TiO_{2-x}$**: Sodium hypophosphite monohydrate ($NaH_2PO_2 \cdot H_2O$, 15 mg) was ground in a mortar, and then successively added titanium dioxide ($TiO_2$, commercial P25 100 mg), triruthenium dodecacarbonyl ($Ru_3(CO)_{12}$, 30 mg) and potassium chloroplatinate ($K_2PtCl_4$ 2 mg) to grind 10 minutes to obtain light yellow powder. Afterwards, the yellow powder was put into the quartz porcelain boat and added 60 μL deionized water. Put the quartz porcelain boat into the microwave oven at 700 W for 1 minute to get the black solid. The black solid was added into 30 mL deionized water, and then stirred at 300 rpm for 45 minutes. Finally, it was filtered and dried in a vacuum oven at 60 °C for 6 h to get the black solid powder of Ru/Pt-$TiO_2$ (Pt loading of 0.55%, Ru loading of 2.26%).

## Physical Characterizations

Physical characterizations of the involved catalyst materials were performed by X-ray diffraction (XRD) (Japan Rigaku Ultima IV), Raman spectroscopy (D-MAX 2500/PC), scanning electron microscopy (SEM) (Regulus 8100), transmission electron microscopy (TEM) (JEM-F200), X-ray photoelectron spectroscopy (XPS) (America Thermo Scientific K-Alpha), electron paramagnanetic resonance (EPR) (BRUKE EMXPLUS), Ultraviolet–visible spectroscopy (UV-vis) (Agilent 730), and Inductively Coupled Plasma (ICP) (Hitachi U4150).

## Electrochemical Measurements

Measurements of Ru-Pt/P-$TiO_{2-x}$ catalysts were carried out using a three-electrode structure with carbon rod, reversible hydrogen electrode (RHE), and glassy carbon electrode (5 mm diameter) as counter electrode, reference electrode, and working electrode, respectively. A total of 5 mg of catalyst and 1 mg of carbon black were dispersed in 20 μL of Nafion solution (Shanghai, China, 5 wt%) in isopropanol solution (1 mL) and then sonicated for 30 minutes to form a homogeneous ink. Then, 20 μL of ink was dropped onto a glassy carbon electrode (containing 0.05 mg of catalyst). Measurement of the HER performance of the catalyst was carried out separately in a 0.5 M $H_2SO_4$ medium. The measured linear sweep voltammetry curves were swept at

a rate of 5 mV $s^{-1}$ and tested for stability at specific potentials. For comparison, commercial Pt/C and Ru/C catalysts, as well as Ru-Pt/P-$TiO_{2-x}$, were also prepared by this method, and all electrochemical tests were carried out at room temperature.

## TOF calculation

$$total\ hydrogen\ turnovers = (|j|\frac{mA}{cm^2})(\frac{\frac{1C}{s}}{1000\ mA})(\frac{1\ mol\ e^-}{96485.3\ C})(\frac{1\ mol}{2\ mol\ e^-})(\frac{6.022\times10^{23}\ molecules\ H_2}{1\ mol\ H_2})$$

$$= 3.12\times10^{15}\frac{H_2/s}{cm^2}\text{per}\frac{mA}{cm^2}$$

Ru - P$t/P-TiO_{2-x}$ (active sites)

$$= \left(\frac{\text{catalyst loading per geometric area } \times \left(\frac{g}{cm^2}\right) \times \text{Ru wt\%}}{\text{Ru } M_W\left(\frac{g}{mol}\right)}\right)\left(\frac{6.022\times10^{23}\text{Ru atomes}}{1\text{ mol Ru}}\right)$$

$$= \left(\frac{0.05\times\frac{10^{-3}g}{cm^2}\times 0.0226\text{ wt\%}}{101.1}\right)\left(\frac{6.022\times10^{23}\text{Ru atomes}}{1\text{ mol Ru}}\right)$$

$$= 3.42\times10^{18}\text{ Ru sites per cm}^2$$

Ru - P$t/P-TiO_{2-x}$ (active sites)

$$= \left(\frac{\text{catalyst loading per geometric area } \times \left(\frac{g}{cm^2}\right) \times \text{Pt wt\%}}{\text{Pt } M_W\left(\frac{g}{mol}\right)}\right)\left(\frac{6.022\times10^{23}\text{Pt atomes}}{1\text{ mol Pt}}\right)$$

$$= \left(\frac{0.05\times\frac{10^{-3}g}{cm^2}\times 0.00554\text{ wt\%}}{195.084}\right)\left(\frac{6.022\times10^{23}\text{Pt atomes}}{1\text{ mol Pt}}\right)$$

$$= 4.357\times10^{18}\text{ Pt sites per cm}^2$$

$$\mathrm{TOF} = \left(\frac{3.12 \times 10^{15}}{3.42 \times 10^{18}} \times |\mathrm{j}|\right) + \left(\frac{3.12 \times 10^{15}}{4.357 \times 10^{18}} \times |\mathrm{j}|\right) = 1.63 \times 10^{-4} \times |-189.962| = 0.031$$

Ru - $Pt/P-TiO_{2-x}$ (active sites) = $3.1\times10^{-2}$ Ru (Pt) sites per $cm^2$

$Ru/P-TiO_{2-x}$ (active sites) = $2.9\times10^{-5}$ Ru sites per $cm^2$

Ru/C (active sites) = $3.1\times10^{-5}$ Ru sites per $cm^2$

Pt/C (active sites) = $7.4\times10^{-5}$ Pt sites per $cm^2$

**0.5 M $H_2SO_4$:** When the overpotential is 100 mV, the current density j of Ru-Pt/P-$TiO_{2-x}$ is 69 mA $cm^{-2}$, TOF=0.031 $H_2$ $S^{-1}$. Similarly, the current density of Pt/C at 100 mV is 134 mA $cm^{-2}$ and TOF = 0.000073 $H_2$ $S^{-1}$, Ru/C at 100 mV is 374 mA $cm^{-2}$ and TOF = 0.000031 $H_2$ $S^{-1}$, Ru/P-$TiO_2$ at 100 mV is 141 mA $cm^{-2}$ and TOF = 0.000029 $H_2$ $S^{-1}$.

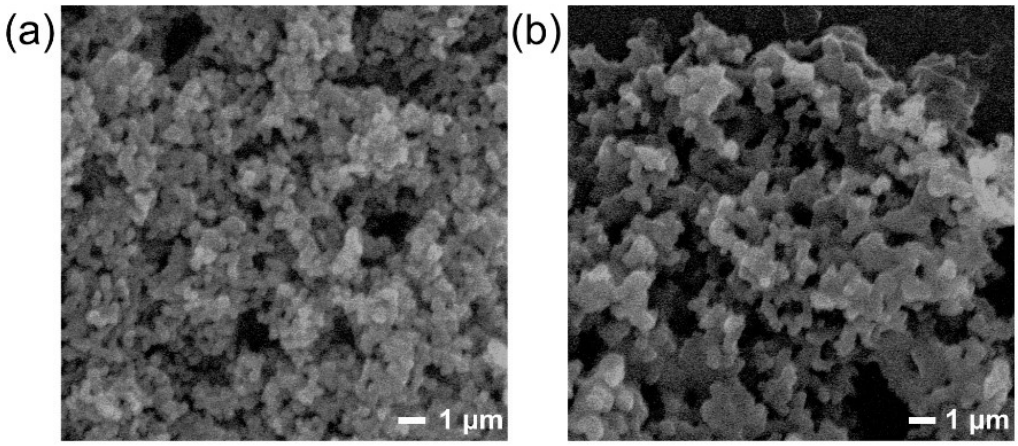


**Figure S1.** SEM images of (a) $TiO_2$ and (b) Ru-Pt/P-$TiO_{2-x}$.

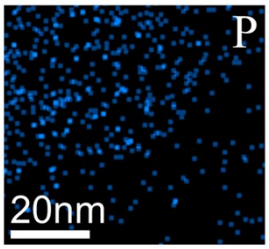


**Figure S2.** EDX elemental mappings of P in Ru-Pt/P-$TiO_{2-x}$.

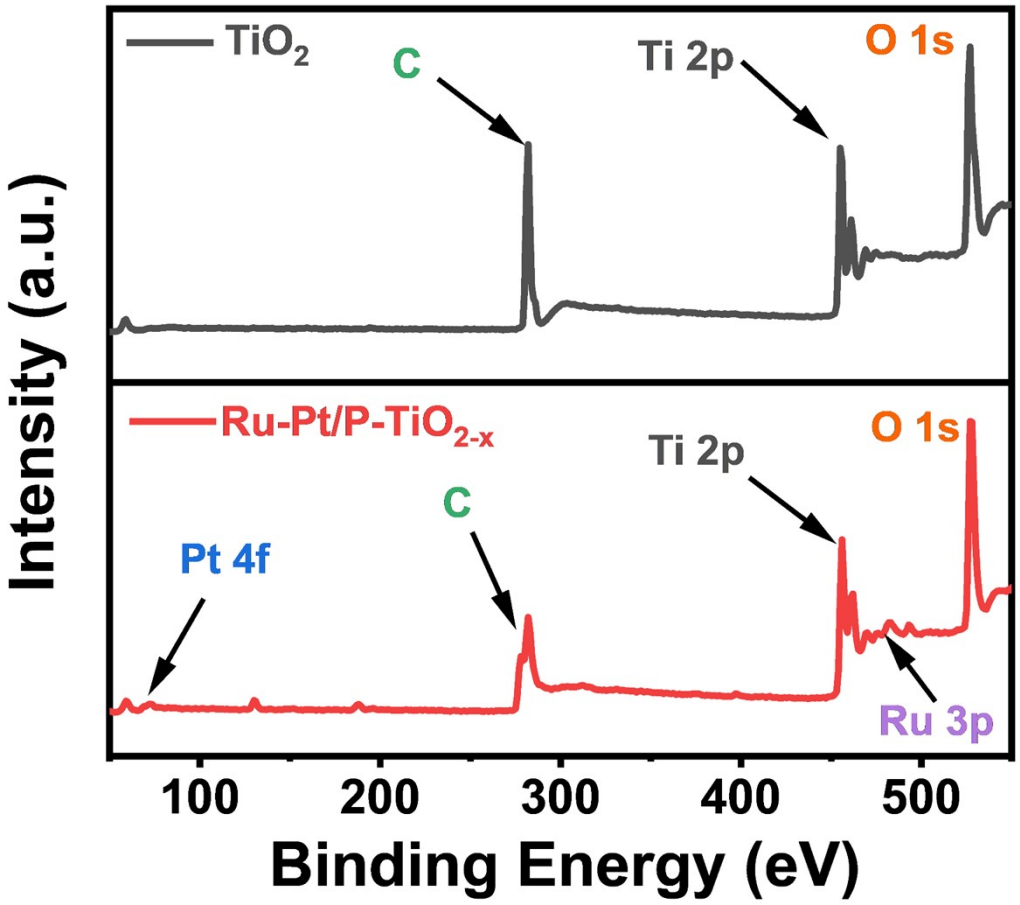


**Figure S3.** XPS analysis of $TiO_2$ and Ru-Pt/P-$TiO_{2-x}$.

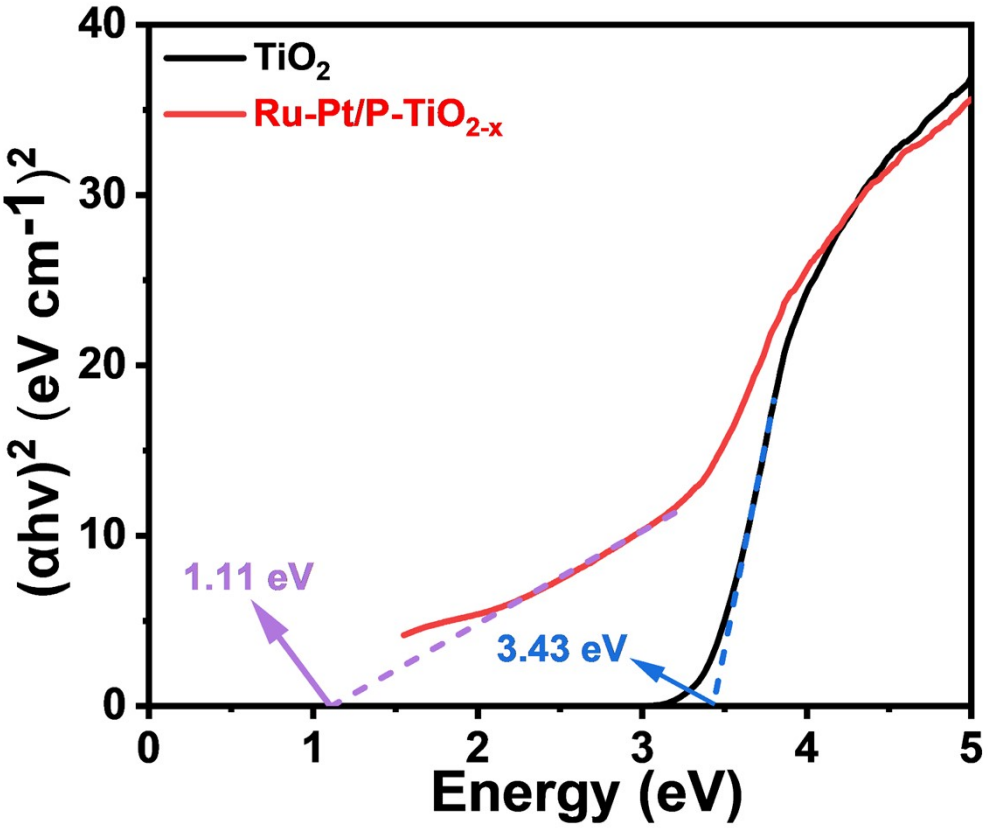


**Figure S4.** Tauc plot of $TiO_2$ and Ru-Pt/P-$TiO_{2-x}$.

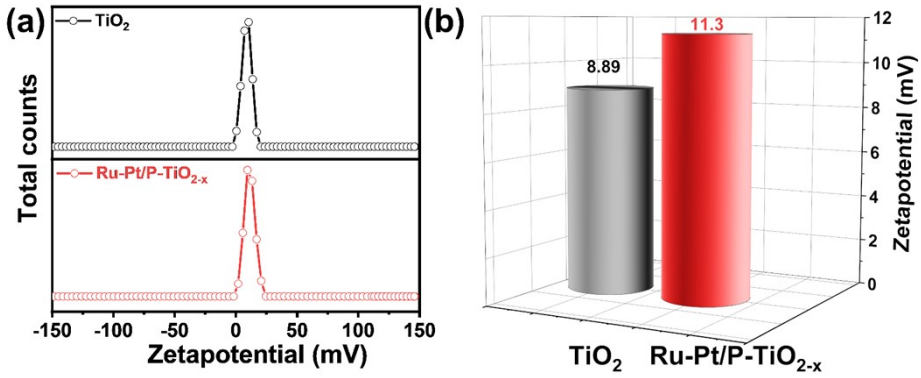


**Figure S5.** (a) Zeta distribution data and (b) zeta potentials of $TiO_2$ and Ru-Pt/P-$TiO_{2-x}$ in 0.5 M $H_2SO_4$.

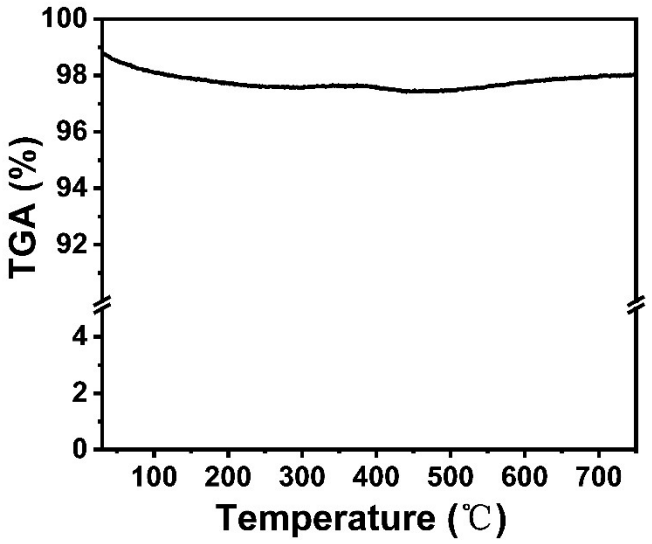


**Figure S6.** TGA curve of Ru-Pt/P-$TiO_{2-x}$.

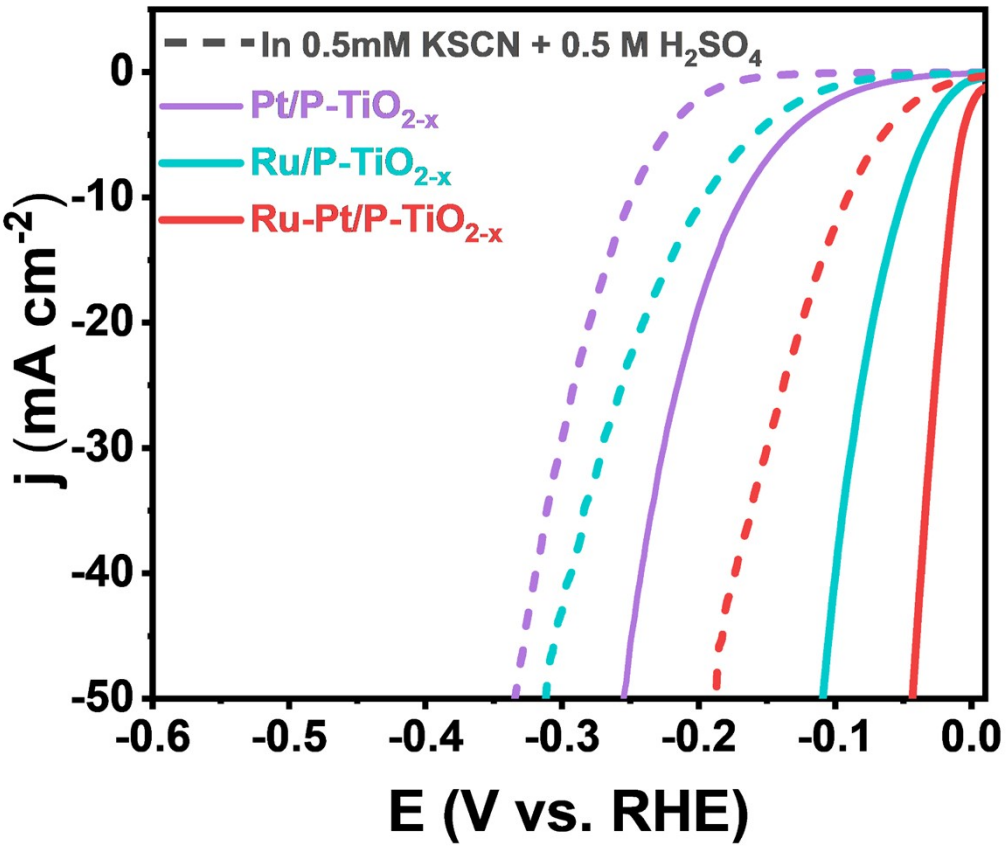


**Figure S7.** LSVs curves of Pt/P-$TiO_{2-x}$, Ru/P-$TiO_{2-x}$, Ru-Pt/P-$TiO_{2-x}$ catalysts in 0.5 mM KSCN + 0.5 M $H_2SO_4$.

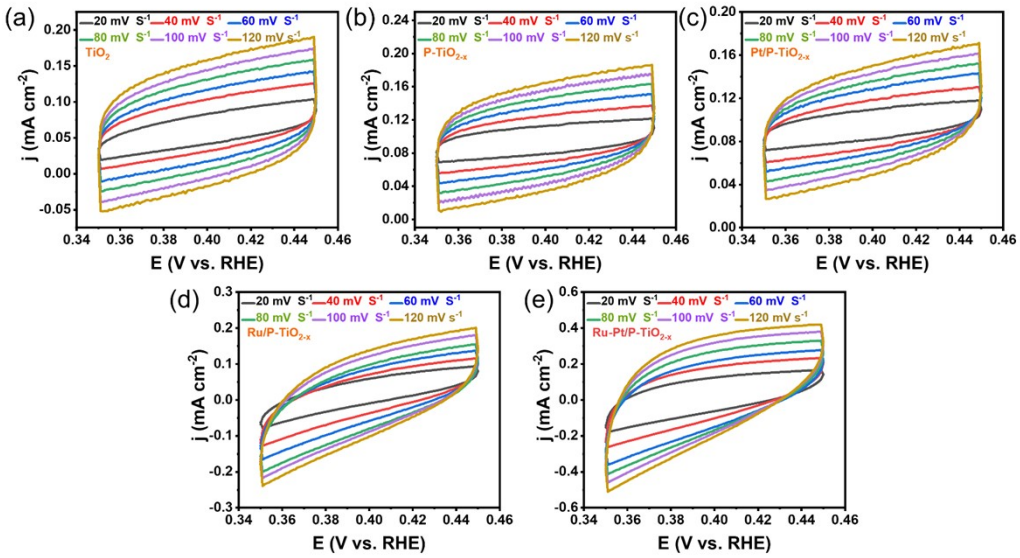


**Figure S8.** Cyclic voltammograms of (a) $TiO_2$, (b) P-$TiO_{2-x}$, (c) Pt/P-$TiO_{2-x}$, (d) Ru/P-$TiO_{2-x}$ and (e) Ru-Pt/P-$TiO_{2-x}$ in the region of 0.35~0.45 V vs. RHE at different scan rates in 0.5 M $H_2SO_4$.

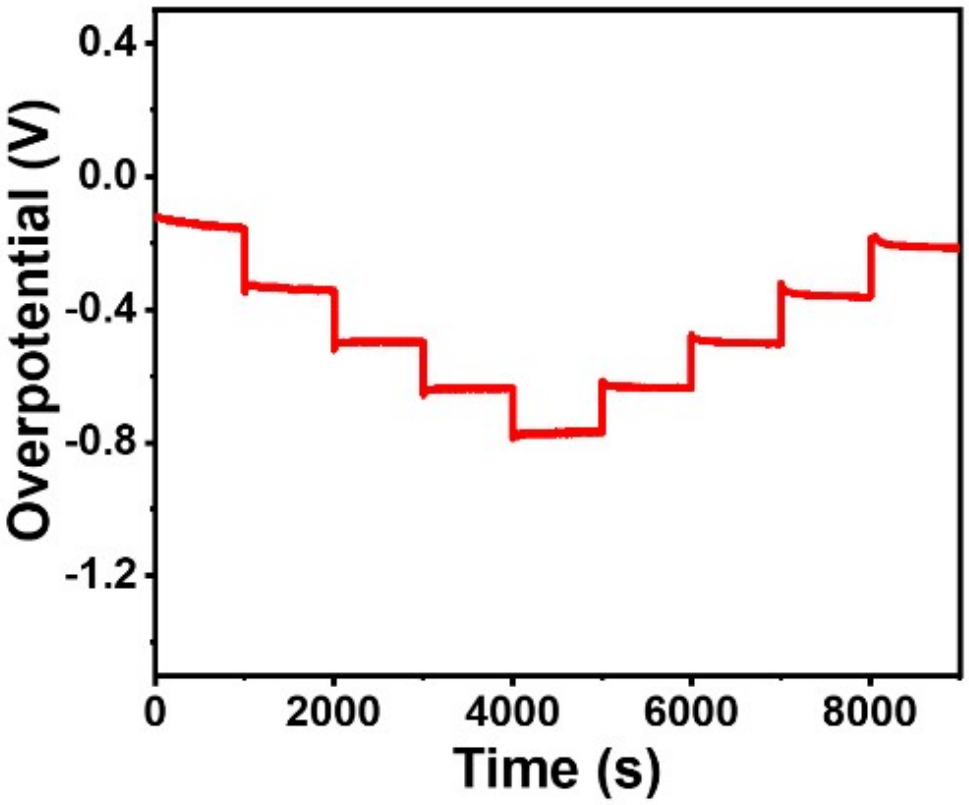


**Figure S9.** Multi-step Chronopotentiometry testing of Ru-Pt/P-$TiO_{2-x}$ in 0.5 M $H_2SO_4$.

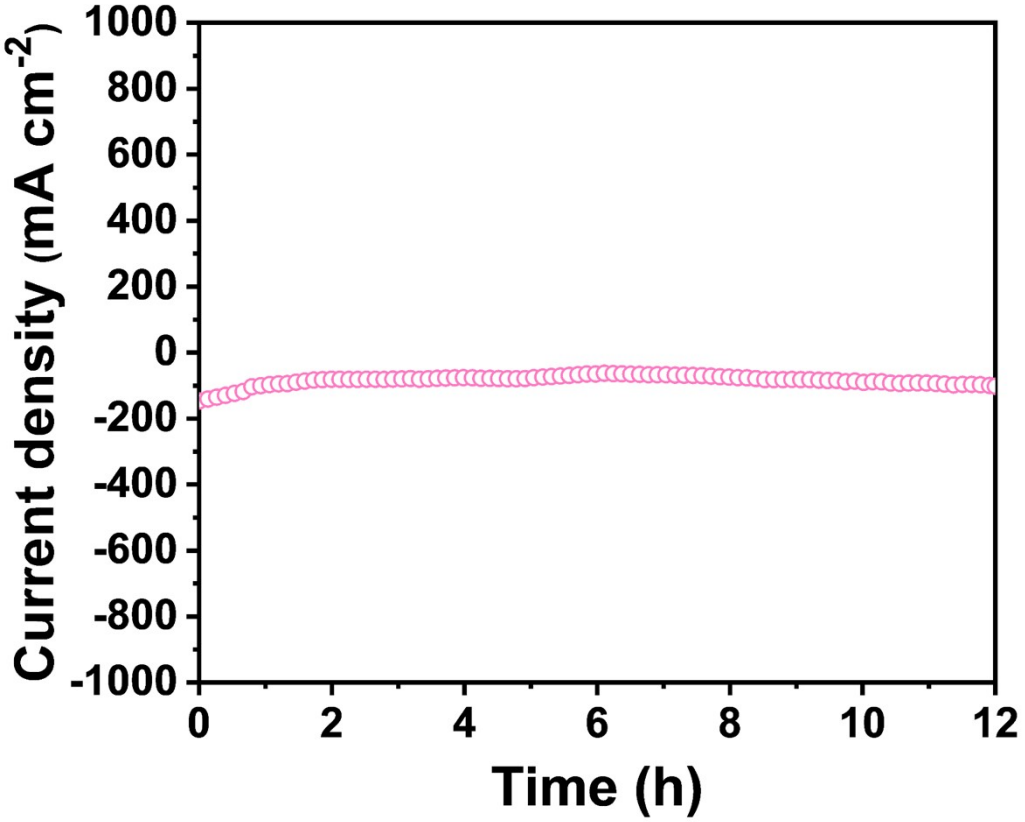


**Figure S10.** The chronoamperometric curves for Ru-Pt/P-$TiO_{2-x}$ at 100 mA $cm^{-2}$ in 0.5 M $H_2SO_4$.

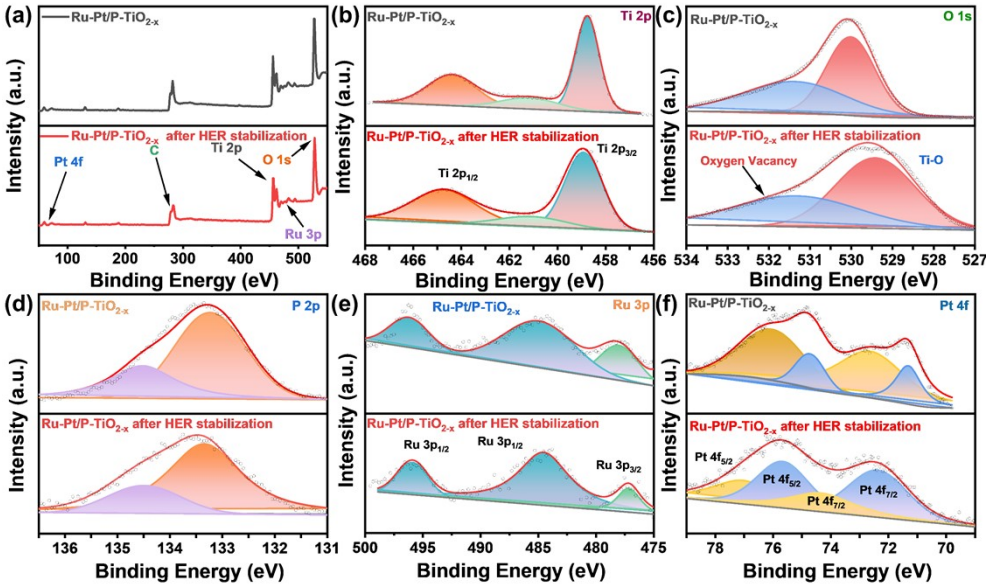


**Figure S11.** (a) XPS spectra in Ru-Pt/P-$TiO_{2-x}$ and Ru-Pt/P-$TiO_{2-x}$ after HER stabilization, XPS spectra of (b) Ti 2p, (c) O 1s, (d) P 2p, (e) Ru 3p and (f) Pt 4f in Ru-Pt/P-$TiO_{2-x}$ and Ru-Pt/P-$TiO_{2-x}$ after HER stabilization.

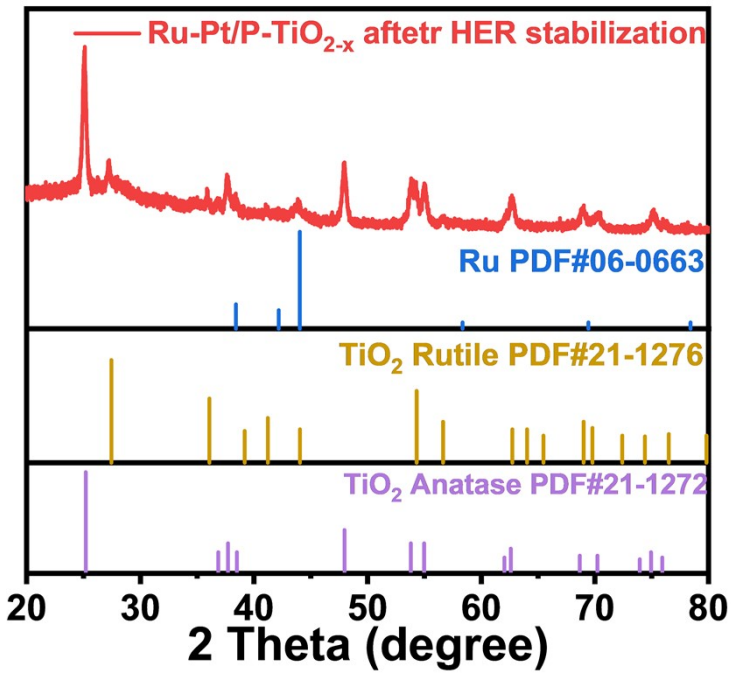


**Figure S12.** XRD of Ru-Pt/P-$TiO_{2-x}$ after HER stabilization.

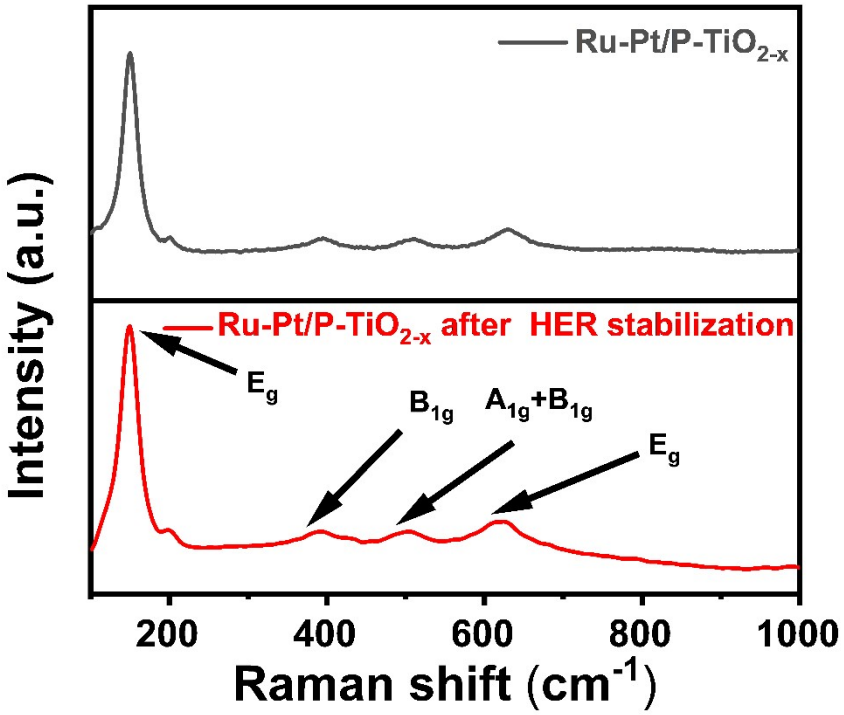


**Figure S13.** Raman spectrum of Ru-Pt/P-$TiO_{2-x}$ and Ru-Pt/P-$TiO_{2-x}$ after HER stabilization.

**Table S1.** Comparison of the HER activity of the Ru/Pt-$TiO_2$ with other previously reported electrocatalysts under 0.5 M $H_2SO_4$.

| Catalysts | Electrolyte | $\eta_{10}$ / mV | Tafel / mV $dec^{-1}$ | Ref. |
|---|---|---|---|---|
| RuP(L-RP) | 0.5 M $H_2SO_4$ | 19 | 37 | 1 |
| Ru-NGC | 0.5 M $H_2SO_4$ | 25 | 31 | 2 |
| Pt@DNA | 0.5 M $H_2SO_4$ | 26 | 30 | 3 |
| Ru-CSS | 0.5 M $H_2SO_4$ | 27 | 33 | 4 |
| PtAg NCs | 0.5 M $H_2SO_4$ | 36 | 40 | 5 |
| $Ru^0$ /$TiO_2$ | 0.5 M $H_2SO_4$ | 41 | 52 | 6 |
| Pt/def-$WO_3$@CFC | 0.5 M $H_2SO_4$ | 42 | 61 | 7 |
| $Sr_2RuO_4$ | 0.5 M $H_2SO_4$ | 61 | 51 | 8 |
| Pt-$Mo_2C$ | 0.5 M $H_2SO_4$ | 79 | 55 | 9 |
| Ru/MeOH/THF | 0.5 M $H_2SO_4$ | 83 | 46 | 10 |
| **Ru/Pt-$TiO_2$** | **0.5 M $H_2SO_4$** | **14** | **28** | **This work** |

**References**


1 J. Yu, Y. Guo, S. She, S. Miao, M. Ni, W. Zhou, M. Liu, Z. Shao, Bigger is Surprisingly Better: Agglomerates of Larger RuP Nanoparticles Outperform Benchmark Pt Nanocatalysts for the Hydrogen Evolution Reaction, *Adv. Mater.*, 2018, **30**, 39 1800047.

2 Q. Song, X. Qiao, L. Liu, Z. Xue, C. Huang, T. Wang, Ruthenium@N-doped graphite carbon derived from carbon foam for efficient hydrogen evolution reaction, *Chem. Commun.*, 2019, **55**, 7 965-968.

3 S. Anantharaj, P. E. Karthik, B. Subramanian, S. Kundu, Pt Nanoparticle Anchored Molecular Self-Assemblies of DNA: An Extremely Stable and Efficient HER Electrocatalyst with Ultralow Pt Content, *ACS Catal.*, 2016, **6**, 7 4660-4672.

4 D. Luo, B. Zhou, Z. Li, X. Qin, Y. Wen, D. Shi, Q. Lu, M. Yang, H. Zhou, Y. Liu, Biomimetic organization of a ruthenium-doped collagen-based carbon scaffold for hydrogen evolution, *J. Mater. Chem. A*, 2018, **6**, 5 2311-2317.

5 X. Weng, Q. Liu, A.-J. Wang, J. Yuan, J.-J. Feng, Simple one-pot synthesis of solid-core@porous-shell alloyed PtAg nanocrystals for the superior catalytic activity toward hydrogen evolution and glycerol oxidation, *J. Colloid Interface Sci.*, 2017, **494**, 15-21.

6 E. Demir, S. Akbayrak, A. M. Önal, S. Özkar, Titania, zirconia and hafnia supported ruthenium(0) nanoparticles: Highly active hydrogen evolution catalysts, *J. Colloid Interface Sci.*, 2018, **531**, 570-577.

7 H. Tian, X. Cui, L. Zeng, L. Su, Y. Song, J. Shi, Oxygen vacancy-assisted hydrogen evolution reaction of the Pt/$WO_3$ electrocatalyst, *J. Mater. Chem. A*, 2019, **7**, 11 6285-6293.

8 Y. Zhu, H. A. Tahini, Z. Hu, J. Dai, Y. Chen, H. Sun, W. Zhou, M. Liu, S. C. Smith, H. Wang, Z. Shao, Unusual synergistic effect in layered Ruddlesden−Popper oxide enables ultrafast hydrogen evolution, *Nat. Commun.*, 2019, **10**, 1 149.

9 M. Chen, Y. Ma, Y. Zhou, C. Liu, Y. Qin, Y. Fang, G. Guan, X. Li, Z. Zhang, T. Wang. Influence of Transition Metal on the Hydrogen Evolution Reaction over Nano-Molybdenum-Carbide Catalyst, *Catalysts*, 2018, **8**, 7 294.

10 S. Drouet, J. Creus, V. Collière, C. Amiens, J. García-Antón, X. Sala, K. Philippot, A porous Ru nanomaterial as an efficient electrocatalyst for the hydrogen evolution reaction under acidic and neutral conditions, *Chem. Commun.*, 2017, **53**, 85 11713-11716.